

Hydrogen termination of CVD diamond films by high-temperature annealing at atmospheric pressure

V. Seshan,^{1,2} D. Ullien,¹ A. Castellanos-Gomez,² S. Sachdeva,¹ D. H. K. Murthy,¹ T. J. Savenije,¹ H. A. Ahmad,¹ T. S. Nunney,³ S. D. Janssens,^{4,5} K. Haenen,^{4,5} M. Nesládek,^{4,5} H. S. J. van der Zant,² E. J. R. Sudhölter,¹ and L. C. P. M. de Smet^{1,a)}

¹*Department of Chemical Engineering, Delft University of Technology, Julianalaan 136, 2628 BL Delft, The Netherlands*

²*Kavli Institute of Nanoscience, Delft University of Technology, Lorentzweg 1, 2628 CJ Delft, The Netherlands*

³*Thermo Fisher Scientific, Unit 24, The Birches, Imberhorne Lane, East Grinstead, West Sussex RH19 1UB, United Kingdom*

⁴*Institute for Materials Research (IMO), Hasselt University, Wetenschapspark 1, BE-3590 Diepenbeek, Belgium*

⁵*IMOME, IMEC vzw, Wetenschapspark 1, BE-3590 Diepenbeek, Belgium*

(Received 10 April 2013; accepted 29 May 2013; published online 21 June 2013)

A high-temperature procedure to hydrogenate diamond films using molecular hydrogen at atmospheric pressure was explored. Undoped and doped chemical vapour deposited (CVD) polycrystalline diamond films were treated according to our annealing method using a H₂ gas flow down to ~50 ml/min (STP) at ~850 °C. The films were extensively evaluated by surface wettability, electron affinity, elemental composition, photoconductivity, and redox studies. In addition, electrografting experiments were performed. The surface characteristics as well as the optoelectronic and redox properties of the annealed films were found to be very similar to hydrogen plasma-treated films. Moreover, the presented method is compatible with atmospheric pressure and provides a low-cost solution to hydrogenate CVD diamond, which makes it interesting for industrial applications. The plausible mechanism for the hydrogen termination of CVD diamond films is based on the formation of surface carbon dangling bonds and carbon-carbon unsaturated bonds at the applied temperature, which react with molecular hydrogen to produce a hydrogen-terminated surface. © 2013 AIP Publishing LLC. [<http://dx.doi.org/10.1063/1.4810866>]

I. INTRODUCTION

Diamond is an extraordinary material due to its distinctive bulk properties such as the highest thermal conductivity, extreme hardness, broad optical transparency, bio-compatibility, chemical inertness, and excellent electrical insulation, which can be tailored to become semiconducting or normal conducting by doping with boron.^{1,2} As a result, diamond materials have been used in different applications ranging from micromechanical oscillators in acoustics to heat-sinks in radio-frequency devices and also from coatings of cutting tools to transistors in electronic devices.^{1,2}

In addition to the above-mentioned superior bulk properties, the surface of diamond exhibits interesting properties too. For example, the type of surface termination affects the surface conductivity and electron affinity properties. In more detail, hydrogen-terminated diamond shows *p*-type surface conductivity with a negative electron affinity, whereas oxygen-terminated diamond shows surface-insulating properties with a positive electron affinity.³ The change of surface termination of diamond (O-terminated vs. H-terminated) is reversible and controllable, which has created a niche market for diamond-based sensor devices that include biosen-

sors, ion-sensitive field effect transistors, and electrochemical sensors.¹ Oxygen termination of diamond can be done by contacting the diamond film with a boiling oxidizing acid, by oxygen plasma, by cathodic treatment, or by ultraviolet (UV)/ozone treatment.⁴ Conversely, the hydrogen termination of diamond traditionally has been achieved using atomic hydrogen produced by either plasma or hot filament techniques.⁵ In spite of their popularity, these hydrogenation techniques are not widely available, but more importantly, they also have some drawbacks. Plasma techniques may cause undesired etching of the film, while hot filament techniques can sometimes cause surface contamination that originates from the deposition of the filament material. Although hydrogen termination of diamond was recently achieved also electrochemically, this method can be applied only to doped (i.e., conducting) diamond.⁶ As an alternative to the approaches mentioned above, hydrogenation using molecular hydrogen (H₂) has also been reported but only on undoped single crystal diamond (at ~800 °C and high-vacuum conditions) and aggregated nanodiamond powder (at ~500 °C and low vacuum conditions).⁷ Nevertheless, the requirement of the vacuum condition increases considerably the cost of the technique and constraints on the wafer sizes, hampering industrial application. Therefore, an alternative hydrogenation technique at atmospheric pressure would be highly attractive.

^{a)} Author to whom correspondence should be addressed. Electronic mail: l.c.p.m.desmet@tudelft.nl.

In this work, we show that high-temperature molecular hydrogen can also be applied to hydrogenate the surface of diamond films even at atmospheric pressure. The presented atmospheric-pressure process, unlike high-vacuum techniques, can be easily scaled up to fabricate cost-effective hydrogenated diamond for industry. The focus of this paper is on the demonstration of hydrogenation of both doped and undoped chemical vapour deposited (CVD) diamond films. CVD-prepared diamond films can be grown in a planar and non-planar form on different substrates, making it an interesting material for a wide variety of applications.² We extensively compared the results of our low-cost and highly facile method with the standard hydrogen-plasma technique on the film properties by studying the wettability, electron affinity, and elemental composition of the surface. In addition to surface properties, the optoelectronic and electrical properties of the surface-treated films were investigated.

II. EXPERIMENTAL

Two types of CVD diamond films were used for the experiments to show the versatility of the high-temperature annealing technique. The first type of samples used is undoped nanocrystalline diamond films (~ 150 nm thick with smaller grain size) grown on quartz at Hasselt University. The CVD growth details of this film, including the measurement of the film thickness can be found in Ref. 8. The second type of samples are doped electrochemical grade CVD diamond films (freestanding polycrystalline plates, 0.6 mm thick with larger grain size, resistivity: $0.02\text{--}0.18\ \Omega\ \text{cm}$, boron doping $>10^{20}\ \text{cm}^{-3}$) that were purchased from Element 6 (UK). Each type of film was subjected to three different surface treatments, i.e., (1) UV/ozone treatment (UV/ozone-treated, used for reference purposes), (2) hydrogen-plasma treatment (H plasma-treated, used as a benchmark), and (3) high-temperature annealing treatment in molecular hydrogen gas at atmospheric pressure (H_2 -treated, the method presented here). In more detail, oxidation of the films was done under UV light in ambient condition for ~ 4 h using a *UV/Ozone ProCleaner* system (*BioForce Nanosciences Inc.*). H plasma treatment of the films was carried out in a plasma reactor at $\sim 700^\circ\text{C}$ and 3500 W for 5 min. H_2 -treatment of the films was carried out in a non-plasma quartz tube reactor connected with a H_2 gas supply line. The films were heated to $\sim 850^\circ\text{C}$ under H_2 gas (99.999% purity) flow. The films were kept for 20 min at $\sim 850^\circ\text{C}$ followed by cooling down to room temperature under a continuous H_2 gas flow. During the entire H_2 -treatment, the H_2 gas flow was typically maintained at ~ 525 ml/min (STP) under atmospheric pressure. Additionally, we found that the H_2 -treatment can also be carried out with a H_2 gas flow as low as ~ 50 ml/min (STP), a factor of 10 less than the previous flow rate, under atmospheric pressure. Notice that the results shown in the present article correspond to samples hydrogenated with a H_2 gas flow rate of ~ 525 ml/min (STP), but similar results were obtained for samples hydrogenated with ~ 50 ml/min (STP). All the films were UV/ozone-treated as an intermediate step before changing from H_2 -treatment to H plasma treatment and vice versa. This intermediate step was performed as a reset step to differentiate the results ob-

tained from H_2 -treated and H plasma-treated film. To study the influence of above treatments on surface and electronic properties, the films were subjected to different characterization techniques.

The surface wettability was studied with an *Easy Drop* goniometer (*Krüss GmbH*, Germany) at room temperature. Pictures of the droplets were taken immediately after dispensing $1\ \mu\text{l}$ of MilliQ water on the sample and were subsequently analyzed using drop-shape analysis software. The measurements were taken at 11 different spots on the film to obtain the average static water contact angle (WCA).

The difference in secondary electron emission of the surface was assessed using scanning electron microscopy (SEM, *FEI Philips XL20*). Before SEM analysis, the H_2 -treated film was partially covered with aluminum foil to protect it from oxidation, while rest of the film was oxidized under UV light. After UV/ozone treatment, the foil was removed to obtain two different, well-separated areas with different surface terminations on the same film to study their secondary electron emission as reflected by the difference in relative contrast of the image.

The elemental analysis of CVD diamond surfaces that were exposed to ambient conditions up to several days was carried out using an X-ray Photoelectron Spectrometer (XPS, *Thermo Fisher Scientific*, *K Alpha* model). A monochromated Al K_α X-ray source was used. XPS measurements were taken in normal emission with a spot size of $400\ \mu\text{m}$ at a base pressure of 10^{-9} mbar. During all XPS measurements the flood gun was enabled to compensate for the potential charging of surfaces. C 1s region scans were averaged over 10 scans and taken at 50 eV pass energy. The spectra were analyzed using *Avantage* processing software. The XPS spectra were background corrected using the “Smart” base line function available in the software, and peak fitting was done using a Gaussian (70%)-Lorentzian (30%) convolution function.

The electrical characterization of a undoped CVD film using a 2-probe technique was carried out to measure the surface resistance (see supplementary material, Sec. 1).⁹

The optoelectronic properties of differently treated films were evaluated by measuring the photoconductivity using the electrodeless Time-Resolved Microwave Conductivity (TRMC) technique. Using this technique, the change in conductance of the film, on photo-excitation is recorded on tens of nanoseconds time scale without applying any external electrodes. A home-built TRMC setup consists of an X-band (8.45 GHz) microwave cell. Diamond films were photo-excited with a 3 ns laser pulse from an optical parametric oscillator pumped by a Q-switched Nd:YAG laser (*Vibrant II*, *Opotek*). Photo-generation of mobile charge carriers in the film leads to an increase of the conductance, $\Delta G(t)$, and consequently to an enhanced absorption of microwave power by the sample. The time-dependent change of the conductance is obtained from the normalized change in microwave power ($\Delta P(t)/P$) reflected from the cell and is given by Eq. (1):

$$\Delta P(t)/P = -K \Delta G(t). \quad (1)$$

The geometrical dimensions of the cavity and dielectric properties of the media in the microwave cavity determine the sensitivity factor, K . The change in conductance is related to the

number of photo-generated electrons and holes and the sum of their mobilities determined using the following equation: $\Delta G_{\max}/\beta e I_0 F_A$. Here, β is the ratio between the broad and narrow internal dimensions of the microwave cell, e is the electronic charge, I_0 is the incident light intensity, and F_A is the fraction of incident light absorbed by the film. A detailed discussion related to this technique can be found in Refs. 10 and 11.

The redox properties of the doped films were measured using cyclic voltammetry (CV, *Electrochemical analyzer/CH Instruments*). For CV measurements, the diamond film was used as a working electrode with the current polarity setting as “cathodic positive,” a standard calomel electrode (SCE) as a reference electrode, and a platinum wire as a counter electrode. The sample was mounted in a Teflon cell with an O-ring of 0.25 cm² area, ensuring that the analysis areas for all electrochemical experiments were identical in size. The back contact was achieved via InGa eutectic. An electrolyte solution of 1M KNO₃ with 2 mM Fe(CN)₆^{3-/4-} redox couple was used and the scan rate was 20 mV/s. Note that it has been reported that the electrochemical behavior of the Fe(CN)₆^{3-/4-} redox couple is very sensitive to the surface termination of the diamond electrode, making it an ideal redox couple for our study.¹² To further study the reactivity of the H₂-treated diamond film, surface modification was performed using the electrochemical reduction of a diazonium salt. Dodecyldiazonium tetrafluoroborate was prepared by the standard method from the corresponding aniline with NaNO₂ in tetrafluoroboric acid.¹³ A solution of 2.5 mM dodecyldiazonium tetrafluoroborate in 25 mM of tetrabutylammonium tetrafluoroborate in acetonitrile was added to the cell and electrografting experiments were carried out at a scan rate of 50 mV/s. This experiment was also performed using an UV/ozone-treated diamond sample.

The undoped and doped films were characterized using WCA analysis, SEM, XPS, and TRMC. In addition, the doped films were also characterized using CV.

III. RESULTS AND DISCUSSION

In the first part of the results section data acquired from surface characterization techniques such as WCA, SEM, and XPS are discussed to compare the results of different treatments on the surface of the film. For clarity, the WCA and SEM results of undoped samples are discussed here. The results obtained from the doped film were similar to those of the undoped films (see supplementary material, Sec. 2).⁹ The second part deals with the influence of surface treatment on the optoelectronic and redox properties of the film. The focus of the last part is on electrografting experiments.

The measurement of WCAs provides a quick and easy way to evaluate the relative hydrophilicity or hydrophobicity of surfaces. WCAs are of particular practical value in the case of switching from oxygen-terminated surfaces to hydrogen-terminated surfaces as these surfaces are hydrophilic and hydrophobic, respectively.¹⁴ Figures 1(a) and 1(b) show a drop of water on the UV/ozone-treated and the H₂-treated film, respectively. The WCA for the UV/ozone-treated CVD diamond film was found to be ~15°, while the WCA of the

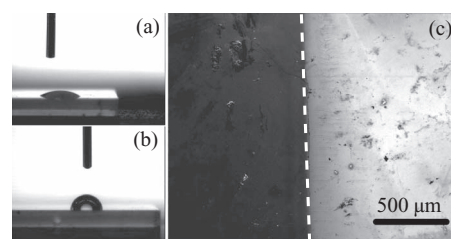


FIG. 1. Water contact angle on (a) UV/ozone-treated and (b) H₂-treated undoped CVD diamond film. (c) SEM image of the undoped CVD diamond film showing two domains with a difference in contrast due to a difference in secondary electron emission. The dashed line (guide to the eye) indicates the boundary between the UV/ozone-treated and H₂-treated portion on the same film.

H₂-treated film was ~83°, which agrees well with the values obtained on H plasma-treated film (~84°) and reported values in the literature.¹⁵ These results show that the H plasma and H₂-treatment at atmospheric pressure produce surfaces with similar hydrophobicity.

Subsequently, CVD diamond films with different surface terminations were studied with SEM. It is known that—in contrast to oxidized diamond surfaces—hydrogen-terminated diamond surfaces display strong electron emission.¹⁶ This difference has been attributed to the difference in electron affinity between H and O, which results in a lower energy barrier for electron emission in the case of hydrogen-terminated diamond surfaces. In a SEM image, differences in secondary electron emission are reflected by the difference in contrast, which can also be used to discriminate between oxygen- and hydrogen-terminated domains of a diamond film.^{6,16} Figure 1(c) shows a SEM image of a H₂-treated sample that was partly covered during the oxidation process, resulting in a film with two different domains. In the SEM image, the part of the diamond film that was covered during the oxidation step is much brighter than the other (oxidized) part, suggesting the presence of hydrogen termination in the former case.^{6,16}

Although WCA and SEM studies provide a quick and macroscopic evaluation of relative surface properties, a more detailed analysis is needed to obtain insight into the type of functional groups on the diamond surface. Hence the samples were subsequently analysed with XPS, followed by a peak-fitting procedure (Fig. 2). First, it is observed that the C 1s spectra of the H plasma-treated and H₂-treated diamond films are similar to each other, but different from the one of the UV/ozone-treated sample. In more detail, all spectra show peaks at ~284.0 and ~285.0 eV (peak I and II, respectively), which are indicative for photoelectrons from non-oxidized C 1s. As oxidized and hydrogenated CVD films are only different in terms of the interfacial atoms, most of the electrons probed by XPS are related to bulk C—C present in the top 5–10 nm. The difference in peak position of bulk C—C in the XPS spectra of oxidized and hydrogenated CVD films (~285.0 and ~284.0 eV, respectively) can be explained by the difference in band bending in these samples. It is known that the hydrogenated diamond film exhibits upward band bending caused by surface Fermi level pinning.^{17,18} This reduces the energy barrier for electron emission from the bulk C—C groups detected by XPS. Hence, the dominant peak is

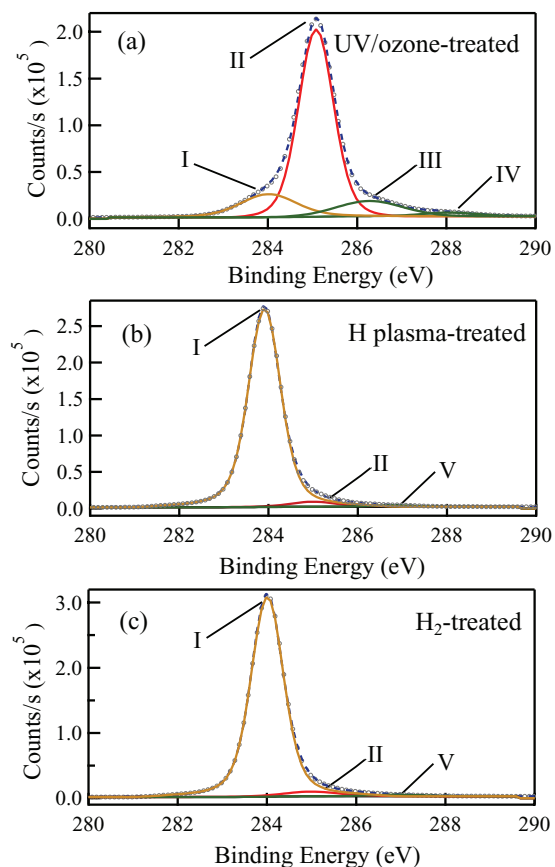


FIG. 2. XPS C 1s region spectra of an undoped CVD diamond film treated with (a) UV/ozone, (b) H plasma and (c) H₂-treatment at $\sim 850^\circ\text{C}$ and atmospheric pressure. The dashed line represents the acquired spectrum; the convoluted peaks (solid lines, labeled as I, II, III, IV, and V) were obtained via peak fitting. The total fit is given by circles. See main text for further details on the peak assignment.

observed at a lower binding energy (~ 284.0 eV) in Figs. 2(b) and 2(c). Upon oxidation, the Fermi level position at the diamond surface is modified leading to an increase in the energy barrier for electron emission and consequently shifting the bulk C–C peak to ~ 285.0 eV. This explanation suggests that the oxidized sample is not fully oxidized as Fig. 1(a) shows a peak at both positions. The contribution ~ 284.0 eV in Fig. 1(a) may originate from sub-surface areas that are not fully exposed to the ozone treatment and/or it may be related to surface roughness. Angle-resolved XPS may give more information on this issue. Also, the hydrogenated surfaces contain traces of oxidized carbon, but in those cases the peak I/peak II area ratio is comparable (28.4 and 25.5 for Figs. 2(b) and 2(c), respectively). The subpeaks at a binding energy > 285 eV (peak III, IV, and V) can be assigned to photoelectrons from oxidized C 1s.^{6,18} Figure 2(a) shows subpeaks at 286.3 (peak III) and 288.1 eV (peak IV), which can be assigned to C–O and C=O, respectively.⁶ In the case of the hydrogenated samples only one subpeak related to oxidized C 1s is observed (peak V at ~ 286.8 eV, $< \sim 4\%$ of all C 1s photoelectrons). The survey scans revealed the presence of oxygen (O 1s) and silicon (Si 1s) in all three cases, which we attribute to SiO₂ residues from the quartz tube reactor (see supplementary material, Sec. 3).⁹ However, the residue problem due to

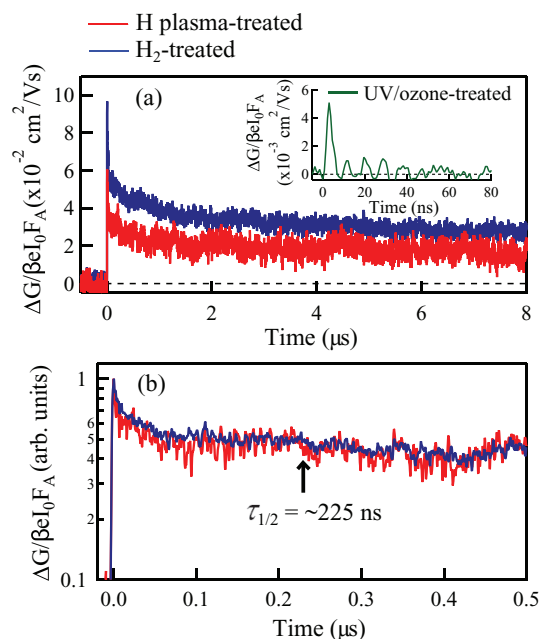


FIG. 3. (a) Photoconductance transient for H plasma-treated (red curve) and H₂-treated (blue curve) undoped CVD diamond film measured using the TRMC technique. The insert shows the photoconductance transient of UV/ozone-treated (green curve) film. (b) Normalized photoconductance transient showing charge carrier lifetime data. The arrow indicates the half-life ($\tau_{1/2}$).

quartz tube could be overcome by using high-temperature, resistant alloy tube reactors.

In summary, the XPS analysis shows that the chemical composition of the hydrogenated diamond films is very similar.

The following part focuses on the effect of the surface treatment on the optoelectronic and electrical properties of CVD diamond films. To study the influence of surface treatment on the optoelectronic properties of the film, photoconductivity measurements were carried out using the electrodeless TRMC technique. This technique has been used to study the charge transport properties, i.e., charge carrier mobility and charge carrier lifetime in semiconductor materials such as silicon.^{10,19} Figure 3(a) shows the photoconductance transients obtained on pulsed excitation for the H plasma-treated (red curve) and H₂-treated (blue curve) film at 300 nm wavelength and 0.18 mJ/cm² incident intensity. Since the TRMC technique is electrodeless, the decay of the conductance is due to charge carrier recombination or trapping of mobile carriers. The intensity-normalized photoconductance magnitudes, corresponding to $\Delta G_{\max}/\beta e I_0 F_A$, for H plasma-treated and H₂-treated diamond films were found to be similar and amount to ~ 0.06 cm²/Vs and ~ 0.09 cm²/Vs, respectively. Figure 3(b) shows the photoconductance transients normalized to unity for the H plasma-treated (red curve) and H₂-treated (blue curve) film on a shorter time scale. For both samples the half-life ($\tau_{1/2}$) of the photo-generated charges was found to be ~ 225 ns as extracted from the decay of photoconductance transients. The similar decay kinetics suggest that both the charge carrier generation and recombination in the H₂-treated and H plasma-treated film follow the same photo-physical

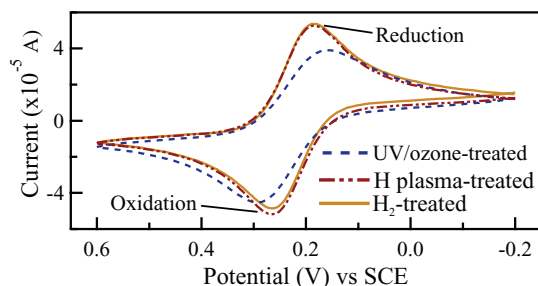


FIG. 4. Cyclic voltammograms of UV/ozone-treated (dashed curve), H plasma-treated (dotted-dashed curve), and H_2 -treated (solid curve) doped CVD diamond film at a scan rate of 20 mV/s. In all cases $\text{Fe}(\text{CN})_6^{3-/4-}$ was used as a redox couple.

pathways. On the contrary, the $\tau_{1/2}$ of the photo-generated mobile charge carriers for UV/ozone-treated film is much shorter (~ 140 ps, insert in Fig. 3(a)) as deduced from the decay of photoconductance transient. The shorter $\tau_{1/2}$ could be attributed to the surface states introduced by oxygen termination in the bandgap region of the film leading to the trapping of mobile charges.²⁰ It is important to note that these differences are only observed when using undoped diamond films (data for the doped film is presented in the supplementary material, Sec. 4)⁹ as the optoelectronic properties of doped films are dominated by bulk conduction.

To conclude this paragraph, the TRMC measurements show that also the opto-electronic properties of H_2 -treated and H plasma-treated CVD diamond films are similar. A detailed investigation on the photoconductance mechanism in the hydrogen- and oxygen-terminated diamond films using the TRMC technique is currently being carried out and will be addressed separately.

To explore the effect of surface treatment on the electrochemical properties of the $\text{Fe}(\text{CN})_6^{3-/4-}$ redox analyte, doped CVD diamond films were used as a working electrode in CV measurements. Unlike TRMC, this technique requires the presence of dopants. Figure 4 shows cyclic voltammograms of an UV/ozone-treated (dashed curve), a H plasma-treated (dotted-dashed curve), and a H_2 -treated (solid curve) diamond films. The oxidation peak indicates oxidation of ferrocyanide ($\text{Fe}(\text{CN})_6^{4-}$) to ferricyanide ($\text{Fe}(\text{CN})_6^{3-}$), whereas the reduction peak implies the reversed reaction (Fig. 4). The direction of the shift of the redox peak positions upon UV/ozone-treatment is in line with literature if one takes into account the difference in current polarization (in our case “cathodic positive”).^{6,12} The UV/ozone-treated and H_2 -treated film show oxidative to reductive peak potential separation (ΔE_p) of 132 mV and 80 mV, respectively. The observation that H_2 -treated films give a lower ΔE_p value in comparison to the UV/ozone-treated film is also in agreement with literature.^{6,12} The lower value of ΔE_p is an indication of a faster electron transfer process and more reversible behaviour.^{12,21} The difference in ΔE_p values related to the two different terminations has been attributed to the improved electronic interaction between the $\text{Fe}(\text{CN})_6^{3-/4-}$ redox couple and the hydrogen-terminated diamond surface.¹² In addition, the H_2 -treated film shows higher current peak values suggesting increased electrochemical activity unlike the UV/ozone-

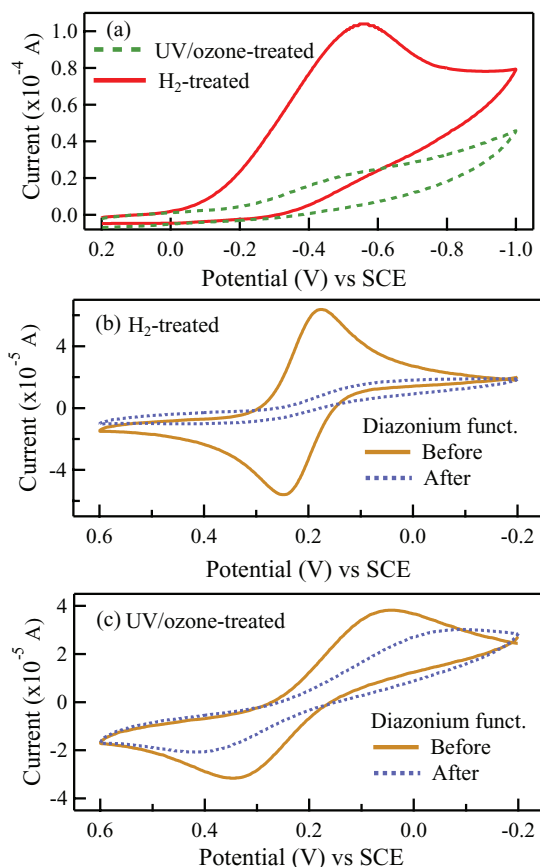


FIG. 5. (a) Cyclic voltammogram of electrografting of 2.5 mM dodecyl-diazonium tetrafluoroborate in acetonitrile on H_2 -treated (solid line) and UV/ozone-treated (dashed line) doped CVD diamond film at a scan rate of 50 mV/s. Cyclic voltammograms of (b) H_2 -treated and (c) UV/ozone-treated doped CVD diamond film before (solid curve) and after (dotted curve) diazonium functionalization at a scan rate of 20 mV/s. In the case of (b) and (c) $\text{Fe}(\text{CN})_6^{3-/4-}$ was used as a redox couple.

treated film. The redox peaks of the H plasma-treated film overlap with those of H_2 -treated film, suggesting a similar type of electron transfer kinetics for both systems. Finally, it is observed that the formal reduction potential (E^0) determined by $(E_p^{\text{ox}} + E_p^{\text{red}})/2$, is about 226 ± 1 mV in all three cases. The obtained E^0 value is in agreement with the reported values for ferro-/ferricyanide couple taking into account the type of reference electrode, concentration of potassium ions, and nature of anions present.²²

The CV results clearly indicate a difference in the redox activity of UV/ozone-treated and H_2 -treated/H plasma-treated film, whereas an almost indistinguishable difference between H_2 -treated and H plasma-treated film suggests a similar type of surface termination.

Finally, the applicability of the H_2 -treated film is shown by grafting it with aryl groups via the electrochemical reduction of a diazonium salt.^{23,24} Figure 5(a) (solid line) shows the cyclic voltammogram of the electrochemical attachment of dodecylphenyl groups to the H_2 -treated diamond surface. The peak at -0.56 V is attributed to the electroreduction. This value is higher than the reported value of the nitro-substituted phenyl diazonium salt,²³ which can be readily understood by difference in the electronegativity of the functional group:

NO₂ is an electron-withdrawing group, making it easier to electrograft as compared to an alkyl-substituted phenyl diazonium. As diazonium salts are reported to be reactive to OH-terminated diamond as well,²³ we also repeated our grafting experiment on UV/ozone-treated NCD as well (Fig. 5(a), dashed line). It is observed that the current amplitude of the latter plot is ~4 times as low as compared to the plot of the H₂-treated film, which is in line with the literature.²³ From Figs. 5(b) and 5(c) it becomes clear that the redox activity of Fe(CN)₆^{3-/4-} is reduced for both electrografting experiments. These results show that diamond films treated with molecular hydrogen at high temperature and atmospheric conditions can be derivatized electrochemically with organic functionalities.

IV. CONCLUSION

A high-temperature annealing procedure using molecular hydrogen at atmospheric pressure was explored as an alternative method to hydrogenate diamond films. Along with the surface properties also the optoelectronic and redox characteristics of the annealed films were found to be very similar to the properties of diamond films that were hydrogen-plasma treated. The work indicates the presence of chemisorbed hydrogen atoms on the surface after the treatment with H₂ at ~850 °C and atmospheric pressure. As H₂ does not dissociate thermally at ~850 °C, the hydrogenation can be rationalized on the basis of the thermal dissociation of surface functional groups.²⁵ This dissociation would subsequently result in the formation of active surface sites, e.g., carbon dangling bonds and carbon-carbon unsaturated bonds.²⁶ These sites can then dissociate molecular hydrogen, leading to the formation of C–H bonds, analogous to what has been reported for the thermally induced hydrogenation of diamond powders.²⁷ Further it has been shown that diazonium salts can be electrografted onto the H₂-treated diamond films. The reference grafting experiment using a UV/ozone-treated diamond surface showed a lower reduction amplitude, indicating that less molecules grafted onto this surface. Based on this difference we conclude that C–H bonds have been formed as hydrogenated diamond has proven to be more reactive towards the electrochemical grafting of diazonium salts as compared to oxidized diamond.²³

The presented hydrogenation method can be used for both undoped and doped CVD diamond and does not require high vacuum conditions, making it a cost-effective and an easily accessible alternative to hydrogenate diamond films.

ACKNOWLEDGMENTS

We thank Duco Bosma (Delft University of Technology) for a fruitful discussion on the analysis of the SEM data. This work was supported by the Delft University of Technology, Hasselt University, the Research Programs G.0555.10N of the Research Foundation-Flanders (FWO), the European Union (FP7) through the programs RODIN, MOLESOL, and the Marie Curie ITN “MATCON” (PITN-GA-2009-238201).

- ¹R. S. Sussmann, *CVD Diamond for Electronic Devices and Sensors* (Wiley, 2009).
- ²R. S. Balmer, J. R. Brandon, S. L. Clewes, H. K. Dhillon, J. M. Dodson, I. Friel, P. N. Inglis, T. D. Madgwick, M. L. Markham, T. P. Mollart, N. Perkins, G. A. Scarsbrook, D. J. Twitchen, A. J. Whitehead, J. J. Wilman, and S. M. Woollard, *J. Phys.: Condens. Matter* **21**, 364221 (2009).
- ³F. Maier, J. Ristein, and L. Ley, *Phys. Rev. B* **64**, 165411 (2001); F. Maier, M. Riedel, B. Mantel, J. Ristein, and L. Ley, *Phys. Rev. Lett.* **85**, 3472–3475 (2000).
- ⁴M. Wang, N. Simon, C. Decorse-Pascanut, M. Bouttemy, A. Etcheberry, M. S. Li, R. Boukherroub, and S. Szunerits, *Electrochim. Acta* **54**, 5818–5824 (2009); Y. Mori, H. Kawarada, and A. Hiraki, *Appl. Phys. Lett.* **58**, 940–941 (1991).
- ⁵H. Kawarada, *Surf. Sci. Rep.* **26**, 205–259 (1996); A. Lafosse, M. Bertin, S. Michaelson, R. Azria, R. Akhvediani, and A. Hoffman, *Diamond Relat. Mater.* **17**, 949–953 (2008).
- ⁶R. Hoffmann, A. Kriele, H. Obloh, J. Hees, M. Wolfer, W. Smirnov, N. Yang, and C. E. Nebel, *Appl. Phys. Lett.* **97**, 052103 (2010).
- ⁷F. Fizzotti, A. Lo Giudice, C. Manfredotti, C. Manfredotti, M. Castellino, and E. Vittone, *Diamond Relat. Mater.* **16**, 836–839 (2007); O. A. Williams, J. Hees, C. Dieker, W. Jager, L. Kirste, and C. E. Nebel, *ACS Nano* **4**, 4824–4830 (2010).
- ⁸S. D. Janssens, S. Drijckoningen, M. Saitner, H. G. Boyen, P. Wagner, K. Larsson, and K. Haenen, *J. Chem. Phys.* **137**, 044702 (2012).
- ⁹See supplementary material at <http://dx.doi.org/10.1063/1.4810866> for surface conductivity measurements, water contact angle measurements, a micro-droplet condensation experiment, SEM images for doped and undoped diamond samples for different H₂ gas flow treatments, survey XPS spectra of UV/ozone-, H plasma-, H₂-treated and as received diamond samples, and TRMC data on a doped sample.
- ¹⁰T. J. Savenije, P. van Veenendaal, M. P. de Haas, J. M. Warman, and R. E. I. Schropp, *J. Appl. Phys.* **91**, 5671–5676 (2002).
- ¹¹J. E. Kroeze, T. J. Savenije, M. J. W. Vermeulen, and J. M. Warman, *J. Phys. Chem. B* **107**, 7696–7705 (2003).
- ¹²M. C. Granger and G. M. Swain, *J. Electrochem. Soc.* **146**, 4551–4558 (1999).
- ¹³B. S. Furniss, A. J. Hannaford, V. Rogers, P. W. G. Smith, and A. R. Tatchell, *Vogel's Textbook of Practical Organic Chemistry, Including Qualitative Organic Analysis*, 4th ed. (Longman, London/New York), 1978), p. 687.
- ¹⁴Y. Kaibara, K. Sugata, M. Tachiki, H. Umezawa, and H. Kawarada, *Diamond Relat. Mater.* **12**, 560–564 (2003); L. Ostrovskaia, V. Perevertailo, V. Ralchenko, A. Dementjev, and O. Loginova, *ibid.* **11**, 845–850 (2002).
- ¹⁵M. Geisler and T. Hugel, *Adv. Mater.* **22**, 398–402 (2010); F. Pinzari, P. Ascarelli, E. Cappelli, G. Mattei, and R. Giorgi, *Diamond Relat. Mater.* **10**, 781–785 (2001).
- ¹⁶J. B. Cui, J. Ristein, M. Stammer, K. Janischowsky, G. Kleber, and L. Ley, *Diamond Relat. Mater.* **9**, 1143–1147 (2000).
- ¹⁷D. Ballutaud, N. Simon, H. Girard, E. Rzepka, and B. Bouchet-Fabre, *Diamond Relat. Mater.* **15**, 716–719 (2006).
- ¹⁸M. Wang, N. Simon, G. Charrier, M. Bouttemy, A. Etcheberry, M. S. Li, R. Boukherroub, and S. Szunerits, *Electrochem. Commun.* **12**, 351–354 (2010).
- ¹⁹C. Swiatkowski, A. Sanders, K. D. Buhre, and M. Kunst, *J. Appl. Phys.* **78**, 1763–1775 (1995).
- ²⁰J. C. Zheng, X. N. Xie, A. T. S. Wee, and K. P. Loh, *Diamond Relat. Mater.* **10**, 500–505 (2001); W. Deferme, G. Tanasa, J. Amir, K. Haenen, M. Nesladek, and C. F. J. Flipse, *ibid.* **15**, 687–691 (2006).
- ²¹P. T. Kissinger and W. R. Heineman, *J. Chem. Educ.* **60**, 702–706 (1983).
- ²²S. P. Rao, S. R. Singh, and S. R. Bandakavi, *Proc. Indian Natl. Sci. Acad.: Phys. Sci.* **44**, 333–335 (1978).
- ²³N. J. Yang, J. H. Yu, H. Uetsuka, and C. E. Nebel, *Electrochem. Commun.* **11**, 2237–2240 (2009).
- ²⁴H. Uetsuka, D. Shin, N. Tokuda, K. Saeki, and C. E. Nebel, *Langmuir* **23**, 3466–3472 (2007); J. Wang, M. A. Firestone, O. Auciello, and J. A. Carlisle, *ibid.* **20**, 11450–11456 (2004).
- ²⁵I. Langmuir, *J. Am. Chem. Soc.* **34**, 860–877 (1912); F. Jansen, I. Chen, and M. A. Machonkin, *J. Appl. Phys.* **66**, 5749–5755 (1989).
- ²⁶A. C. Ferrari and J. Robertson, *Phys. Rev. B* **64**, 075414 (2001).
- ²⁷C. Manfredotti, P. Bonino, M. De La Pierre, E. Vittone, and C. Manfredotti, *Diamond Relat. Mater.* **19**, 279–283 (2010); T. Ando, M. Ishii, M. Kamo, and Y. Sato, *J. Chem. Soc., Faraday Trans.* **89**, 1783–1789 (1993).